EUROPEAN JOURNAL OF PURE AND APPLIED MATHEMATICS
Vol. 17, No. 3, 2024, 2055-2072
ISSN 1307-5543 – ejpam.com
Published by New York Business Global

Investigating Metric Dimension and Edge Metric Dimension of Hexagonal Boron Nitride and Carbon Nanotubes

Waseem Abbas[1], Faryal Chaudhry[1], Umar Farooq[1,*], Muhammad Azeem[2], Yilun Shang[3]

[1] *Department of Mathematics and Statistics, The University of Lahore, 54000, Pakistan.*
[2] *Department of Mathematics, Riphah International University Lahore, 54000, Pakistan.*
[3] *Department of Computer and Information Sciences, Northumbria University, Newcastle NE1 8ST, UK.*

Abstract. When there is a difference in the distance between two vertices in a simple linked graph, then a vertex x resolves both u and v. If at least one vertex in S distinguishes each pair of distinct vertices in G, then a set S of vertices in G is referred to as a resolving set. G's metric dimension is the minimum number of vertices required in a resolving set. A subset S of vertices in a simple connected graph is called an edge metric generator if each vertex can tell any two distinct edges e_1 and e_2 apart by their respective distances from each other. The edge metric dimension (EMD), denoted as $\dim_e(G)$, is the smallest cardinality of such a subset S that serves as an edge metric generator for G. The primary objective of this study is to investigate the edge metric dimension (EMD) of hexagonal boron nitride and carbon nanotube structures.

2020 Mathematics Subject Classifications: 05C85, 05C90, 05C62,05C12, 05C76

Key Words and Phrases: Metric generator, metric basis, edge metric dimension, hexagonal boron nitride, and carbon nanotube.

1. Introduction

An edge set E and a vertex set V create a simple connected graph G. It can be expressed as (V, E). The quantity of edges that separate any two vertices in V, a_1 and a_2, is their distance, or $d(a_1, a_2)$. If the distances from a vertex v to a_1 and a_2 differ, then that particular vertex v in V may discriminate between the two vertices a_1 and a_2. If every pair of different vertices in G is distinguished by at least one element of S, then

*Corresponding author.
DOI: https://doi.org/10.29020/nybg.ejpam.v17i3.5295

Email addresses: dmat02211001@student.uol.edu.pk (W. Abbas), faryal.chaudhry@math.uol.edu.pk (F. Chudhary),70126471@student.uol.edu.pk (U. Farooq),azeemali7009@gmail.com (M. Azeem), yilun.shang@northumbria.ac.uk (Y. Shang)

every subset S of V is a resolving set of G. The number of items in a metric basis, or a resolving set with a minimal cardinality, is known as the MD of G, or $\dim(G)$.

The minimal of the distances from v to a_1 and a_2 for a vertex v in V and an edge e connecting vertices a_1 and a_2 in E defines the distance between v and e, symbolized as $d(e, v)$. If there are distinctions between the distances from a vertex x to two edges e_1 and e_2, then x in V may distinguish between them. If every pair of unique edges in a connected graph G is distinguished by at least one vertex in S, then the subset S with the fewest vertices in G is the edge resolving set for that graph. The term "EMD" (represented by the symbol $dim_e(G)$) refers to the minimum cardinality of an edge resolving set for G.

Slater [24] first proposed the creation of MD in 1975. He called metric generators finding sets, addressing the issue of uniquely identifying intruders' positions in networks. Following this, in 1976, Harary and Melter [8] were the first to independently propose the idea of a graph's MD, referring to metric generators as resolving sets. It was proposed that instead of only distinguishing between distinct vertices of a graph using a selected subset of vertices, the same subset could also differentiate between two distinct edges. Kelenc et al. To capture such a notion, [9] generated a new parameter called the EMD. They used graph metrics to identify each edge pair by measuring the graph's separation from its chosen choice of vertices.

The idea of MD has been widely applied in many different scientific fields. Drug discovery and pharmacological activity were linked to the EMD of graphs by Chartrand et al. [5]. A robot's navigation could be moved from Euclidean space to a network structure, according to Khuller et al. [10]. suggesting potential applications of MD in robot navigation. Researchers can learn more about the use of MD in intricate digital games by analyzing mastermind games, which was made possible by Chvatal's investigation of the MD of Hamming graphs [6]. Erdős and Lindström [7, 13] also made assertions about the usefulness of MD in different coin-weighing scenarios. Several theoretical research on graphs have been motivated by resolving sets. Fault-tolerant MD has been investigated in [22, 23], which has applications in sensor networks.

The EMD represents a natural extension of the resolving set concept, prompting readers to explore the literature on MD across various classes of graphs. Ali et al.[4, 16], for example, investigated the MD of cycle-related graphs and Mobius networks. The strong MD of graphs was addressed by Kuziak et al. [12], whereas the MD of cocktail party, Toeplitz, and jellyfish graphs were the subject of Liu et al. [14, 15]. In several cycle-related graphs, Ahmad et al. [1] explored the MD. Since Koam and Ahmad [11] researched the EMD of barycentric subdivisions of Cayley graphs, the EMD has gained popularity in arguments about resolvability. Ahsan et al. [2] and Zhang and Gao [28] both examined the convex polytope graph.

Wheel graph-related chemical structures were studied by Yang et al. [25]. Ali et al. [3] systematically investigated the MD of the wheel, gear, and anti-web wheel networks. In their study [21], Raza and Bataineh investigated the dimensions of metric and edge metrics. Yero (2016) discussed MD definitions and related thoughts while Okamoto et al. (2010) researched local MD. Additional research on EMD may be found in [17, 26]. Mixed MD, satisfying both metric and EMD conditions, has been investigated across

various graph families. For instance, Raza et al. [20] explored mixed MDs in rotationally symmetric graphs, providing exact values. Raza and Ji [18] computed mixed MDs for the generalized Petersen graph P(n, 2), while Raza et al. [19] discussed results on mixed MDs for certain path-related graphs. In general, it is NP-hard to establish a graph's EMD [9]. While Kelenc et al. [9] analyzed graph families where $dim(G) = dim_e(G)$, $dim(G) < dim_e(G)$, and $dim(G) > dime(G)$, there is no general connection between metric and EMDs.

MD and EMD are fundamental concepts in graph theory, each serving important roles in various real-world applications. The MD of a graph determines the smallest set of vertices necessary to uniquely identify all other vertices within the graph. This parameter is essential in network optimization, aiding in the development of efficient routing protocols and fault diagnosis algorithms. By pinpointing critical vertices, network monitoring and control become more effective, enhancing overall resilience and performance. Moreover, applications such as location determination systems benefit from the MD by enabling precise spatial inference and object tracking within graph-based environments.

Similarly, the EMD focuses on identifying the minimum set of edges required to uniquely determine all other edges in a graph. This parameter finds relevance in circuit design and testing, where it helps reduce the number of test points needed to diagnose faults in interconnected electronic circuits. In transportation networks, EMD optimization assists in route planning and traffic management by highlighting critical edges whose failure or congestion significantly impacts network connectivity and flow. In summary, both MD and EMD are vital tools in graph analysis and optimization, contributing to the development of robust and efficient systems across various application domains.

h-BN and CNTs are two remarkable nanomaterials that hold immense importance across multiple scientific disciplines. H-BN, with its unique two-dimensional hexagonal lattice structure composed of alternating boron and nitrogen atoms, exhibits exceptional thermal and chemical stability, making it invaluable in various applications such as high-temperature electronics, lubricants, and as a substrate for graphene-based devices due to its insulating properties. On the other hand, CNTs, cylindrical nanostructures formed by rolled-up graphene sheets, possess extraordinary mechanical strength, thermal conductivity, and electrical properties, rendering them indispensable in fields ranging from nanoelectronics and composite materials to biomedical applications like drug delivery and biosensors. Both h-BN and CNTs represent cutting-edge materials with diverse functionalities, offering enormous potential for technological innovation and advancement across a wide spectrum of industries. Understanding their properties and harnessing their capabilities is crucial for unlocking their full potential in addressing current and future societal challenges.

2. GHexagonal boron nitride (h-BN)

A straightforward linked graph representing the h-BN structure shows how its horizontal and vertical cells are arranged, as seen in Figure 1. The total number of cells is $n \times n$, where n represents the number of horizontal cells. $2n^2 + 4n$ is the computation used

to determine the graph's order, denoted as $O(G)$. BN is the acronym for boron nitride. The cubic and hexagonal covalent $2D$ structures are the two most prominent ones within the boron nitride graph. The hexagonal boron nitride graph is the particular subject of our investigation [27].

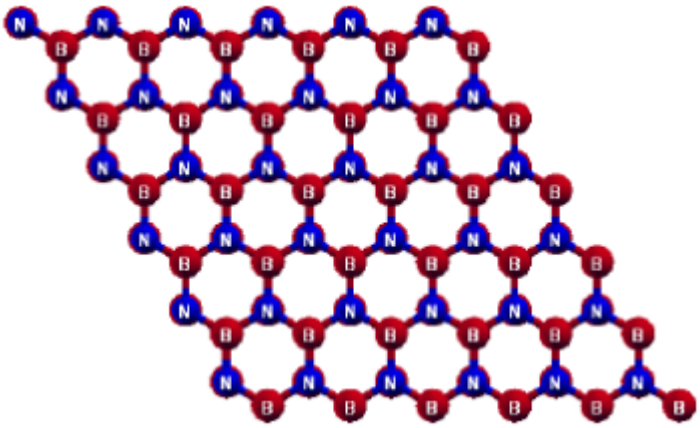

Figure 1. Hexagonal boron nitride

Boron nitride is renowned for its exceptional heat stability, characterized by a low melting point of 3000°C. Its structure consists of a hexagonal arrangement of boron and nitrogen atoms, interconnected alternately. Within this framework, an equal number of boron and nitrogen atoms contribute to the formation of hexagons, with a bond length of 0.145 nm between these atoms. The single-layered hexagonal structure of hexagonal BN is widely utilized due to its notable properties [27]. Understanding the MD and EMD of h-BN is crucial in advancing practical materials and technologies based on this remarkable two-dimensional system. Precisely determining the minimum number of reference points needed to accurately ascertain the locations and distances of all atoms enhances the design and functionality of electronic devices, sensors, and catalysts reliant on h-BN.

This study has the potential to uncover new avenues in materials science, graph theory, and two-dimensional systems. h-BN consists of consecutive boron (B) and nitrogen (N) atoms arranged in a hexagonal lattice structure. Similar to graphite, h-BN possesses a layered architecture where each layer is held together by van der Waals forces, displaying a hexagonal arrangement of atoms.

Theorem 2.1. For the $p \times l$, 2-D lattice $h - BN$ graph, the MD of the hexagonal boron nitride graph is 2.

Proof. In the context of hexagonal boron nitride (h-BN), we are investigating the vertex labeling depicted in the diagram. Moving on, let us consider a $2D$ lattice of h-BN nanotubes of dimensions $p \times l$. The vertex set in this h-BN graph is divided according to this arrangement.

$$\{g_{\xi(1,1)}, g_{\xi(1,2)}, g_{\xi(1,3)}, \ldots, g_{\xi(1,l)}, g_{\xi(2,1)}, g_{\xi(2,2)}, g_{\xi(2,3)}, \ldots, g_{\xi(2,l)},$$

$$g_{\xi(3,1)}, g_{\xi(3,2)}, g_{\xi(3,3)}, \ldots, g_{\xi(3,l)}, \ldots, g_{\xi(p,1)}, g_{\xi(p,2)}, g_{\xi(p,3)}, \ldots, g_{\xi(p,l)}\}$$

Consider $Z = \{g_{\xi(1,1)}, g_{\xi(1,2n+1)}\}$ be a resolving set.

$a_{\eta(\xi)} = 2p$ and $a_n = 2n$.

To indicate the number of rows, vertices in the rows, and cells in the first row, use the symbols p, l, and n.

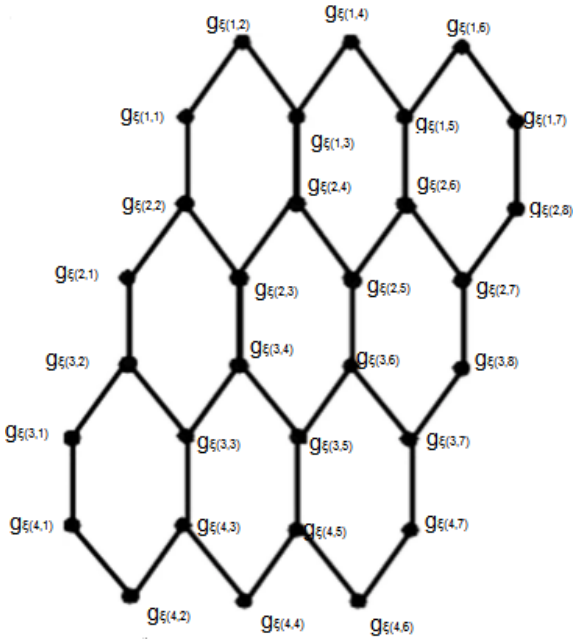

Figure 2. Hexagonal boron nitride graph 3×3

- **Case 1.** If l is odd,

$$r(g_{\xi(p,l)}|Z) = \begin{cases} (a_{\eta(\xi)} - 2, a_n + a_{\eta(\xi)} - (1+l)) & \text{for } 1 \leq l \leq a_{\eta(\xi)} - 1 \\ (l-1, a_n + a_{\eta(\xi)} - (l+1)) & \text{Otherwise} \end{cases}$$

- **Case 2.** If l is even,

$$r(g_{\xi(p,l)}|Z) = \begin{cases} (a_{\eta(\xi)} - 3, a_n + a_{\eta(\xi)} - (1+l)) & \text{for } 1 \leq l \leq a_{\eta(\xi)} - 2 \\ (l-1, a_n + a_{\eta(\xi)} - (l+1)) & \text{Otherwise} \end{cases}$$

For the last row

- **Case 3.** If l is odd,

$$r(g_{\xi(p,l)}|Z) = \begin{cases} (a_{\eta(\xi)} - 3, a_n + a_{\eta(\xi)} - (l+2)) & \text{for } 1 \leq l \leq a_{\eta(\xi)} - 3 \\ (l, a_n + a_{\eta(\xi)} - (2+l)) & \text{Otherwise} \end{cases}$$

- **Case 4.** If l is even,

$$r(g_{\xi(p,l)}|Z) = \begin{cases} (a_{\eta(\xi)} - 2, a_n + a_{\eta(\xi)} - (l+2)) & \text{for } 1 \leq l \leq a_{\eta(i)} - 2 \\ (l, a_n + a_{\eta(\xi)} - (1+l)) & \text{Otherwise} \end{cases}$$

The resolving set Z has a minimum cardinality is two.

Therefore, the h-BN graph's MD is 2.

Theorem 2.2. For the $p \times l$, 2-D lattice $h-BN$ graph, the EMD of the h-BN graph is 2.

Proof.

A graph G has its edges divided into discrete partitions in the following way:

$$\{e_{(1,1)}, e_{(1,2)}, e_{(1,3)}, \ldots, e_{(1,m)}, e_{(2,1)}, e_{(2,2)}, e_{(2,3)}, \ldots, e_{(2,m)},$$
$$e_{(3,1)}, e_{(3,2)}, g_{\xi(3,3)}, \ldots, e_{(3,1)}, \ldots, e_{(i,1)}, e_{(i,2)}, e_{(i,3)}, \ldots, e_{\xi(i,m)}\}$$

Consider $S = \{e_{(1,1)}, e_{(1,2n)}\}$ be a resolving set.

$$a_n = 2n,\ c = i - 2,\ d = m + 1.$$

To indicate the number of rows, vertices in the rows, and cells in the first row, respectively, use the symbols i, m, and n.

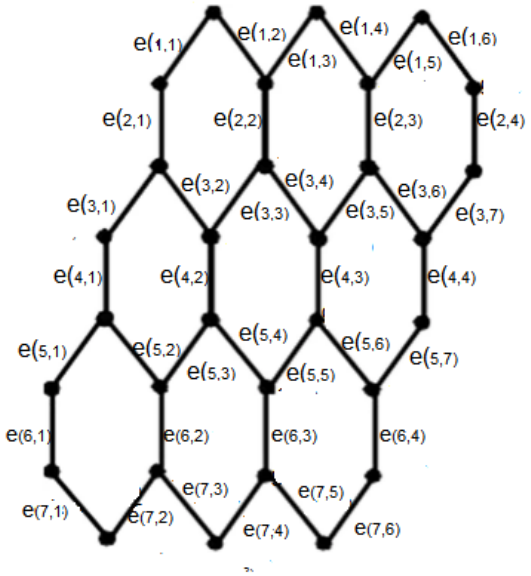

Figure 3. Hexagonal boron nitride graph 3×3

- **Case 1.** If i is odd,

$$r(e_{(i,m)}|S)\begin{cases}(c, a_n + i - d) & \text{for } i > m\\ (m-1, a_n + i - d) & \text{for } i \leq m\end{cases}$$

- **Case 2.** If i is even,

$$r(e_{(i,m)}|S)\begin{cases}(c, a_n + i - 2m) & \text{for } \frac{i}{2} \geq m\\ (E_m, a_n + i - 2m) & \text{for } \frac{i}{2} < m\end{cases}$$

For the last row

- **Case 3.**

$$r(e_{(i,m)}|S) = \begin{cases}(c, a_n - d + i - 1) & \text{for } i \geq m\\ (m, a_n - d + i - 1) & \text{for } i < m\end{cases}$$

A minimum of two cardinality for the resolving set S. So, EMD of the hexagonal boron nitride graph is 2.

3. Carbon nanotubes

The carbon nanotube structure, known as CNT, is shown in Figures 4 and 5 as an easy-to-understand, connected, planar graph. The carbon nanotube graph in Figure 4 consists of a total of $6n^2 + 3n - 2$ edges and $4n^2 + 4n - 1$ vertices. The majority of carbon nanotubes have a diameter of about 1 nanometer, and depending on the particular nanotube structure, the length of the bonds separating carbon atoms as well as the angles between them vary [27].

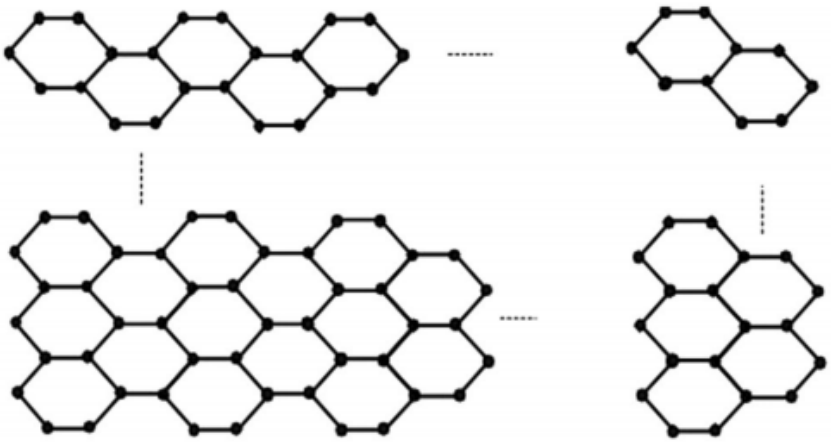

Figure 4. Graph of carbon nanotubes.

Carbon nanotubes are essentially rolled-up sheets of graphene, and their structures are quite complex. To effectively explain a carbon nanotube graph's topological properties and to understand the way it behaves in various uses, its MD must be known. By finding the MD, we can identify a minimal set of atoms or vertices that, when labeled or measured in a specific way, can uniquely identify the location of every other atom in the nanotube. [27].

Theorem 3.1 The MD of $p \times l$, 2-D lattice carbon nanotube is 3.

Proof. The following is the partition of the vertices of G.

$\{c_{\xi(1,1)}, c_{\xi(1,2)}, \ldots, c_{\xi(1,l)}, c_{\xi(2,1)}, c_{\xi(2,2)}, c_{\xi(2,3)}, \ldots, c_{\xi(2,l)}, c_{\xi(3,1)}, c_{\xi(3,2)}, c_{\xi(3,3)}, \ldots, c_{\xi(3,l)}, \ldots, c_{\xi(p,1)}, c_{\xi(p,2)}, c_{\xi(p,3)}, \ldots, c_{\xi(p,l)}\}$

Let $T = \{c_{\xi(1,1)}, c_{\xi(1,2n+1)}, c_{\xi(2n,2n+1)}\}$ be a resolving set.

Number of columns are denoted by p, vertices by l, and number of cells in first column by n.

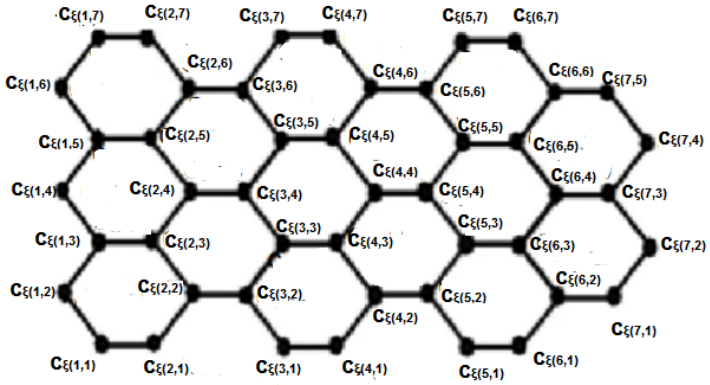

Figure 5. Graph of carbon nanotubes with $n = 3$.

Here we suppose that

$$a_{\eta(n)} = 2n, \qquad a_{\eta(i)} = 2p,$$
$$h = p + l, \qquad b = p - l.$$

- **Case 1.** If p and l both are odd.

$$r(c_{\xi(p,l)}|T) = \begin{cases} (h-2, a_{\eta(n)}+b, 2a_{\eta(n)}-h+1) & \text{for } p=1, l=1 \\ (h-2, a_{\eta(n)}+b, 2a_{\eta(n)}-h-1) & \text{for } p=1, l=3,5,7,\ldots \\ (a_{\eta(i)}-2, a_{\eta(n)}+b, 2a_{\eta(n)}-h+1) & \text{for } p=3, l=1,3 \\ (h-2, a_{\eta(n)}+b, 2a_{\eta(n)}-a_{\eta(i)}-1) & \text{for } p=3, l=5,7,9\ldots \\ (a_{\eta(i)}-2, a_{\eta(n)}+b, 2a_{\eta(n)}-h+1) & \text{for } p \geq l \\ (h-2, a_{\eta(n)}+b, 2a_{\eta(n)}-h+1) & \text{for } p < l \\ (h-2, a_{\eta(i)}-2, 2a_{\eta(n)}-a_{\eta(i)}-1) & \text{for } h \geq a_{\eta(i)+1} \end{cases}$$

- **Case 2.** If p is odd and l is even.

$$r(c_{\xi(p,l)}|T) = \begin{cases} (h-2, a_{\eta(n)}+b, 2a_{\eta(n)}-a_{\eta(i)}) & \text{for } p=1, l=2,4,6.8,\ldots \\ (h-2, a_{\eta(n)}+b, 2a_{\eta(n)}-a_{\eta(i)+2}) & \text{for } p=3, l=2 \\ (h-2, a_{\eta(n)}+b, 2a_{\eta(n)}-a_{\eta(i)}) & \text{for } p=3, l=4,6.8,\ldots \\ (a_{\eta(i)}-3, a_{\eta(n)}+b, 2a_{\eta(n)}-h+1) & \text{for } p \geq l \\ (h-2, a_{\eta(n)}+b, 2a_{\eta(n)}-h+1) & \text{for } p < l \\ (h-2, a_{\eta(i)}-3, 2a_{\eta(n)}-a_{\eta(i)} & \text{for } h \geq a_{\eta(i)}+1 \end{cases}$$

- **Case 3.** If p is even and l is odd.

$$r(c_{\xi(p,l)}|T) = \begin{cases} (h-2, a_{\eta(n)}+b, 2a_{\eta(n)}-h+1) & \text{for } p=2, l=1 \\ (h-2, a_{\eta(n)}+b, 2a_{\eta(n)}-a_{\eta(i)}) & \text{for } p=2, l=3,5,7,\ldots \\ (a_{\eta(i)}-3, a_{\eta(n)}+b, 2a_{\eta(n)}-h+1) & \text{for } p=4, l=1,2 \\ (h-2, a_{\eta(n)}+b, 2a_{\eta(n)}-a_{\eta(i)}) & \text{for } p=4, l=3,4,5.\ldots \\ (a_{\eta(i)}-3, a_{\eta(n)}+b, 2a_{\eta(n)}-h+1) & \text{for } p \geq l \\ (h-2, a_{\eta(n)}+b, 2a_{\eta(n)}-h+1) & \text{for } p < l \\ (h-2, a_{\eta(i)}-3, 2a_{\eta(n)}-a_{\eta(i)}) & \text{for } h \geq a_{\eta(i)+1} \end{cases}$$

- **Case 4.** If p and l both are even.

$$r(c_{\xi(p,l)}|T) = \begin{cases} (h-2, a_{\eta(n)}+b, 2a_{\eta(n)}-h+1) & \text{for } p=2, l=2 \\ (h-2, a_{\eta(n)}+b, 2a_{\eta(n)}-a_{\eta(i)}-1) & \text{for } p=2, l=4,6,8,10,\ldots \\ (h-2, a_{\eta(n)}+b, 2a_{\eta(n)}-h+1) & \text{for } p=4, l=2,4,6 \\ (h-2, a_{\eta(n)}+b, 2a_{\eta(n)}-h-1) & \text{for } p=4, l=8,10,12,\ldots \\ (a_{\eta(i)}-2, a_{\eta(n)}+b, 2a_{\eta(n)}-h+1) & \text{for } p \geq l \\ (h-2, a_{\eta(n)}+b, 2a_{\eta(n)}-h+1) & \text{for } p < l \\ (h-2, a_{\eta(i)}-2, 2a_{\eta(n)}-a_{\eta(i)}-1) & \text{for } h \geq a_{\eta(i)+1} \end{cases}$$

- **Case 5.** For the last row

$$r(c_{\xi(p,l)}|T) = \begin{cases} (a_{\eta(i)}-3, a_{\eta(i)}-3, b) & \text{for if } l \text{ is odd} \\ (a_{\eta(i)}-2, a_{\eta(i)}-2, b) & \text{for pf } l \text{ is even} \end{cases}$$

Consequently, the MD of the carbon nanotube remains at 3.

The MD of a carbon nanotube is determined to be 3, signifying that at least three vertices are necessary to uniquely determine the location of any other vertex on the nanotube.

This implies that to efficiently navigate or locate points within the nanotube structure, a minimum of three reference points, or landmarks, are required, showcasing the intricacy of its spatial arrangement and the necessity for a minimal set of coordinates to characterize its topology accurately.

Theorem 3.2
The MD of the carbon nanotube for a $p \times l$, 2-D lattice carbon nanotube is at least 3.

Proof. The divisions of G's vertices are as follows:
$\{c_{\xi(1,1)}, c_{\xi(1,2)}, \ldots, c_{\xi(1,l)}, c_{\xi(2,1)}, c_{\xi(2,2)}, c_{\xi(2,3)}, \ldots, c_{\xi(2,l)}, c_{\xi(3,1)}, c_{\xi(3,2)}, c_{\xi(3,3)}, \ldots, c_{\xi(3,l)}, \ldots, c_{\xi(p,1)}, c_{\xi(p,2)}, c_{\xi(p,3)}, \ldots, c_{\xi(p,l)}\}$
The number of columns is denoted by p, vertices by l, and the number of cells in the first column by n.

Here, we proceed under the assumption that $T = \{a_{(1,1)}, a_{(1,2n+1)}\}$ is the resolving set, assuming an MD of 2. We aim to demonstrate contradictions.

Case	**Vertices**
$n = 2$	$r(e_{(8,1)}\|T) = r(e_{(8,2)}\|T)$
$n = 3$	$r(e_{(10,2)}\|T) = r(e_{(10,3)}\|T)$ $r(e_{(9,4)}\|T) = r(e_{(9,3)}\|T)$ $r(e_{(12,2)}\|T) = r(e_{(12,4)}\|T) = r(e_{(12,6)}\|T)$ $r(e_{(11,1)}\|T) = r(e_{(11,2)}\|T) = r(e_{(11,3)}\|T) = r(e_{(11,4)}\|T) = r(e_{(11,5)}\|T)$
$n = 4$	$r(e_{(11,4)}\|T) = r(e_{(11,5)}\|T)$ $r(e_{(12,2)}\|T) = r(e_{(12,3)}\|T)$ $r(e_{(13,1)}\|T) = r(e_{(13,2)}\|T) = r(e_{(13,4)}\|T) = r(e_{(13,5)}\|T) = r(e_{(13,6)}\|T) = r(e_{(13,7)}\|T)$ $r(e_{(14,2)}\|T) = r(e_{(14,3)}\|T) = r(e_{(14,4)}\|T)$ $r(e_{(16,1)}\|T) = r(e_{(16,2)}\|T) = r(e_{(16,3)}\|T) = r(e_{(16,4)}\|T)$ $r(e_{(17,1)}\|T) = r(e_{(17,2)}\|T) = r(e_{(17,3)}\|T) = r(e_{(17,4)}\|T) = r(e_{(17,5)}\|T) = r(e_{(17,6)}\|T)$
$n = 5$	$r(e_{(13,5)}\|T) = r(e_{(13,6)}\|T)$ $r(e_{(14,3)}\|T) = r(e_{(14,4)}\|T) = r(e_{(14,5)}\|T)$ $r(e_{(15,3)}\|T) = r(e_{(15,4)}\|T) = r(e_{(15,5)}\|T) = r(e_{(15,6)}\|T)$ $r(e_{(16,2)}\|T) = r(e_{(16,4)}\|T) = r(e_{(16,3)}\|T)$ $r(e_{(17,3)}\|T) = r(e_{(17,4)}\|T) = r(e_{(17,5)}\|T) = r(e_{(17,6)}\|T) = r(e_{(17,7)}\|T)$ $r(e_{(18,2)}\|T) = r(e_{(18,3)}\|T) = r(e_{(18,4)}\|T) = r(e_{(18,5)}\|T)$ $r(e_{(19,2)}\|T) = r(e_{(19,4)}\|T) = r(e_{(19,5)}\|T) = r(e_{(19,6)}\|T) = r(e_{(19,7)}\|T) = r(e_{(19,8)}\|T) = r(e_{(19,9)}\|T)$ $r(e_{(20,1)}\|T) = r(e_{(20,2)}\|T) = r(e_{(20,3)}\|T) = r(e_{(20,4)}\|T) = r(e_{(20,5)}\|T)$ $r(e_{(21,1)}\|T) = r(e_{(21,2)}\|T) = r(e_{(21,3)}\|T) = r(e_{(21,4)}\|T) = r(e_{(21,5)}\|T)$

Table 1: Comparison of vertices for different cases

After generalizing, we have

$$\begin{aligned}
r(c_{\xi(2n+1,7)}|T) = r(c_{\xi(2n+1,5)}|T) = r(c_{\xi(2n+1,3)}|T) = r(c_{\xi(2n+1,1)}|T),\\
r(c_{\xi(2n+1,8)}|T) = r(c_{\xi(2n+1,4)}|T) = r(c_{\xi(2n+1,6)}|T) = r(c_{\xi(2n+1,2)}|T),\\
r(c_{\xi(2n,4)}|T) = r(c_{\xi(2n,6)}|T) = r(c_{\xi(2n,2)}|T) = r(c_{\xi(2n,8)}|T),\\
r(c_{\xi(2n,5)}|T) = r(c_{\xi(2n,3)}|T) = r(c_{\xi(2n,1)}|T) = r(c_{\xi(2n,7)}|T),\\
r(c_{\xi(n+3,5)}|T) = r(c_{\xi(n+3,1)}|T) = r(c_{\xi(n+3,3)}|T) = r(c_{\xi(n+3,7)}|T).
\end{aligned}$$

These are contradictions. Hence, the MD of the carbon nanotube is not less than 3.

Theorem 3.3 The EMD of $p \times l$, the 2-D lattice carbon nanotube is 3.

Proof.

The division of G's vertices is as follows.

$\{e_{(1,1)}, e_{(1,2)}, \ldots, e_{(1,m)}, e_{(2,1)}, e_{(2,2)}, \ldots, e_{(2,m)}, e_{(3,1)}, e_{(3,2)}, e_{(3,3)},$
$\ldots, e_{(3,m)}, \ldots, e_{(i,1)}, e_{(i,2)}, \ldots, e_{(i,m)}\}$

let $T = \{e_{(1,1)}, e_{(1,2n)}, e_{(2n+1,n)}\}$ be a resolving set.

The number of columns is denoted by i, vertices by m, and cells by n in the first column.

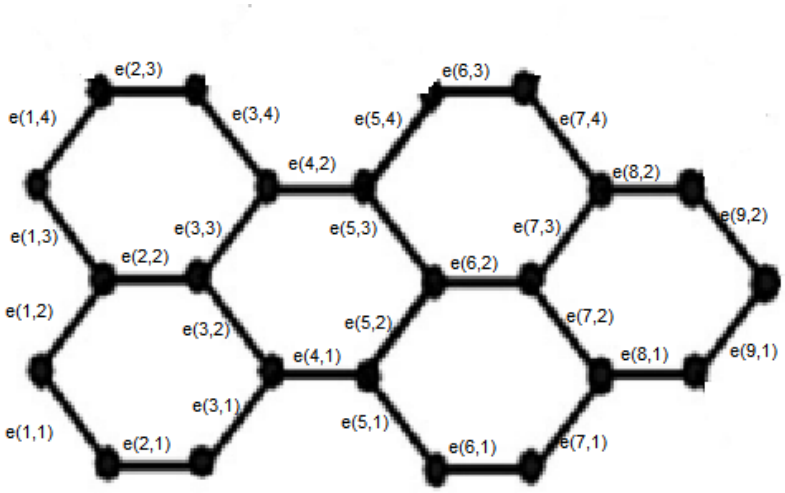

Figure 1: Graph of carbon nanotubes with $n = 2$.

Here, we will organize our discussion of edges based on the line numbers. Initially, we'll focus on lines 1, 5, 9, 13, ...

$$a_{\eta(\xi)} = 2n$$

- **Case 1.**

$i = 1$.

$$r(e_{(i,m)|T}) = \Big\{(i+m-2, 2n-m, 4n-i) \quad \text{for all}$$

$i = 5$.

$$r(e_{(i,m)|T}) = \begin{cases} (i-2, 2n-m+2, 4n-i+1) & \text{for } \frac{i-1}{2} \geq m \\ (m+1, 2n-m+2, 4n-i) & \text{for } \frac{i-1}{2} < m \\ (m+1, i-2, 4n-i) & \text{for } i+m > 2n+5 \end{cases}$$

$i = 9$.

$$r(e_{(i,m)|T}) = \begin{cases} (i-2, 2n-m+4, 4n-i+3) & \text{for } \frac{i-1}{2} \geq m \\ (m+3, 2n-m+4, 4n-i) & \text{for } \frac{i-1}{2} < m \\ (m+3, i-2, 4n-i) & \text{for } i+m > 2n+7 \end{cases}$$

$i = 13$.

$$r(e_{(i,m)|T}) = \begin{cases} (i-2, 2n-m+6, 4n-i+5) & \text{for } \frac{i-1}{2} \geq m \\ (m+5, 2n-m+6, 4n-i) & \text{for } \frac{i-1}{2} < m \\ (m+5, i-2, 4n-i) & \text{for } i+m > 2n+9 \end{cases}$$

We have established the EMD for lines 1, 5, 9, and 13. We will continue this approach to determine the EMD for the subsequent lines in a similar manner.
" We have established the EMD for lines 1, 5, 9, and 13. We will continue this approach to determine the EMD for the subsequent lines in a similar manner.

- **Case 2.**

$i = 2$.

$$r(e_{(i,m)}|T) = \begin{cases} (i-2, 2n-2m+2, 4n-2m) & \text{for } \frac{i}{2} \geq m \\ (2m-2, 2n-2m+2, 4n-i) & \text{for } \frac{i}{2} < m \end{cases}$$

$i = 6$.

$$r(e_{(i,m)}|T) = \begin{cases} (i-2, 2n-2m+4, 2a_{\eta(\xi)}-2m-2) & \text{for } \frac{i+2}{2} \geq m \\ (2m, 2n-2m+4, 2a_{\eta(\xi)}-i) & \text{for } \frac{i+2}{2} < m \\ (2m, i-2, 2a_{\eta(\xi)}-i) & \text{for} i+m \geq 2n \end{cases}$$

$i = 10$.

$$r(e_{(i,m)}|T) = \begin{cases} (i-2, 2n-2m+6, 2a_{\eta(\xi)}-2m-4) & \text{for } \frac{i+2}{2} \geq m \\ (2m+2, 2n-2m+6, 2a_{\eta(\xi)}-i) & \text{for } \frac{i+2}{2} < m \\ (2m+2, i-2, 2a_{\eta(\xi)}-i) & \text{for } i+m \geq 2n+3 \end{cases}$$

$i = 14$.

$$r(e_{(i,m)}|T) = \begin{cases} (i-2, 2n-m+8, 2a_{\eta(\xi)} - 2m + 6) & \text{for } \frac{i+2}{2} \geq m \\ (i-2, 2n-m+8, 2a_{\eta(\xi)} - i) & \text{for } \frac{i+2}{2} < m \\ (2m+4, i-2, 2a_{\eta(\xi)} - i) & \text{for} i+m \geq 2n+6 \end{cases}$$

We have established the EMD for lines 2, 6, 10, and 14. We will continue this approach to determine the EMD for the subsequent lines in a similar manner.

- **Case 3.**

$i = 3$.

$$r(e_{(i,m)}|T) = \Big\{(i+m-3, 2n-m+1, 2a_{\eta(\xi)} - i) \quad \text{for all}$$

$i = 7$.

$$r(e_{(i,m)}|T) = \begin{cases} (i-2, 2n-m+3, 2a_{\eta(\xi)} - m - 4) & \text{for } \frac{i-1}{2} \geq m \\ (m+2, 2n-m+3, 2a_{\eta(\xi)} - i) & \text{for } \frac{i-1}{2} < m \\ (m+2, i-2, 2a_{\eta(\xi)} - i) & \text{for } i+m \geq 2n+4 \end{cases}$$

$i = 11$.

$$r(e_{(i,m)}|T) = \begin{cases} (i-2, 2n-m+5, 2a_{\eta(\xi)} - m - 6) & \text{for } \frac{i-1}{2} \geq m \\ (m+4, 2n-m+5, 2a_{\eta(\xi)} - i) & \text{for } \frac{i-1}{2} < m \\ (m+4, i-2, 2a_{\eta(\xi)} - i) & \text{for } i+m \geq 2n+7 \end{cases}$$

$i = 15$.

$$r(e_{(i,m)}|T) = \begin{cases} (i-2, 2n-m+7, 2a_{\eta(\xi)} - m - 8) & \text{for } \frac{i-1}{2} \geq m \\ (m+6, 2n-m+7, 2a_{\eta(\xi)} - i) & \text{for } \frac{i-1}{2} < m \\ (m+6, i-2, 2a_{\eta(\xi)} - i) & \text{for } i+m \geq 2n+10 \end{cases}$$

We have established the EMD for lines 2, 6, 10, and 14. We will continue this approach to determine the EMD for the subsequent lines in a similar manner.

- **Case 3.** $i = 4$.

$$r(e_{(i,m)}|T) = \Big\{(2m, 2n-2m+2, 2a_{\eta(\xi)} - i) \quad \text{for all}$$

$i = 8$.

$$r(e_{(i,m)}|T) = \begin{cases} (i-2, 2n-2m+4, 2a_{\eta(\xi)} - m - 5) & \text{for } \frac{i}{4} \geq m \\ (2m+2, 2n-2m+4, 2a_{\eta(\xi)} - i) & \text{for} \frac{i}{4} < m \\ (2m+2, i-2, 2a_{\eta(\xi)} - i) & \text{for } i+m \geq 2n+1 \end{cases}$$

$i = 12$.

$$r(e_{(i,m)}|T) = \begin{cases} (i-2, 2n-2m+6, 2a_{\eta(\xi)} - m + 7) & \text{for } \frac{i}{4} \geq m \\ (2m+4, 2n-2m+6, 2a_{\eta(\xi)} - i) & \text{for } \frac{i}{4} < m \\ (2m+4, i-2, 2a_{\eta(\xi)} - i) & \text{for } i+m \geq 2n+4 \end{cases}$$

$i = 16$.

$$r(e_{(i,m)}|T) = \begin{cases} (i-2, 2n-2m+8, 2a_{\eta(\xi)} - m - 9) & \text{for all } \frac{i}{4} \geq m \\ (2m+6, 2n-2m+8, 2a_{\eta(\xi)} - i) & \text{for all } \frac{i}{4} < m \\ (2m+6, i-2, 2a_{\eta(\xi)} - i) & \text{for all } i+m \geq 2n+7 \end{cases}$$

We have established the EMD for lines 4, 8, 12, and 16. We will continue this approach to determine the EMD for the subsequent lines in a similar manner.

The EMD of a carbon nanotube has been identified as 3, indicating that a minimum set of three edges is required to uniquely determine the location of any other edge within the nanotube structure. This finding underscores the complexity of the nanotube's connectivity and highlights the need for a minimal number of edge-based references to fully characterize demonstrating its significance in various computational and graph-theoretical applications.

Theorem 3.2. For the $p \times l$, 2-D lattice $h - BN$ graph, the EMD of the carbon nanotube is not less than 3.

Proof. The EMD of the carbon nanotube in the $p \times l$, 2-D lattice h-BN graph is proven to be not less than 3." I begin by assuming a resolving set with a cardinality of 2, then systematically present contradictions. Subsequently, I will establish that the EMD cannot be 2, thereby concluding that the EMD of the carbon nanotube is 3.

A graph G has its edges divided into discrete partitions in the following way:

$$\{e_{(1,1)}, e_{(1,2)}, e_{(1,3)}, \ldots, e_{(1,m)}, e_{(2,1)}, e_{(2,2)}, e_{(2,3)}, \ldots, e_{(2,m)},$$
$$e_{(3,1)}, e_{(3,2)}, e_{(3,3)}, \ldots, e_{(3,1)}, \ldots, e_{(i,1)}, e_{(i,2)}, e_{(i,3)}, \ldots, e_{(i,m)}\}$$

Consider $S = \{e_{(1,1)}, e_{(1,2n)}\}$

Here, we proceed under the assumption that S is the resolving set, assuming an EMD of 2. Our aim is to demonstrate contradictions.

Case	**Vertices**
$n=2$	$r(e_{(8,1)}\|T)=r(e_{(8,2)}\|T)$
$n=3$	$r(e_{(10,2)}\|T)=r(e_{(10,3)}\|T)$ $r(e_{(9,4)}\|T)=r(e_{(9,3)}\|T)$ $r(e_{(12,2)}\|T)=r(e_{(12,4)}\|T)=r(e_{(12,6)}\|T)$ $r(e_{(11,1)}\|T)=r(e_{(11,2)}\|T)=r(e_{(11,3)}\|T)=r(e_{(11,4)}\|T)=$ $r(e_{(11,5)}\|T)$
$n=4$	$r(e_{(11,4)}\|T)=r(e_{(11,5)}\|T)$ $r(e_{(12,2)}\|T)=r(e_{(12,3)}\|T)$ $r(e_{(13,1)}\|T)=r(e_{(13,2)}\|T)=r(e_{(13,4)}\|T)=r(e_{(13,5)}\|T)=$ $r(e_{(13,6)}\|T)=r(e_{(13,7)}\|T)$ $r(e_{(14,2)}\|T)=r(e_{(14,3)}\|T)=r(e_{(14,4)}\|T)$ $r(e_{(16,1)}\|T)=r(e_{(16,2)}\|T)=r(e_{(16,3)}\|T)=r(e_{(16,4)}\|T)$ $r(e_{(17,1)}\|T)=r(e_{(17,2)}\|T)=r(e_{(17,3)}\|T)=r(e_{(17,4)}\|T)=$ $r(e_{(17,5)}\|T)=r(e_{(17,6)}\|T)$
$n=5$	$r(e_{(13,5)}\|T)=r(e_{(13,6)}\|T)$ $r(e_{(14,3)}\|T)=r(e_{(14,4)}\|T)=r(e_{(14,5)}\|T)$ $r(e_{(15,3)}\|T)=r(e_{(15,4)}\|T)=r(e_{(15,5)}\|T)=r(e_{(15,6)}\|T)$ $r(e_{(16,2)}\|T)=r(e_{(16,4)}\|T)=r(e_{(16,3)}\|T)$ $r(e_{(17,3)}\|T)=r(e_{(17,4)}\|T)=r(e_{(17,5)}\|T)=r(e_{(17,6)}\|T)=$ $r(e_{(17,7)}\|T)$ $r(e_{(18,2)}\|T)=r(e_{(18,3)}\|T)=r(e_{(18,4)}\|T)=r(e_{(18,5)}\|T)$ $r(e_{(19,2)}\|T)=r(e_{(19,4)}\|T)=r(e_{(19,5)}\|T)=r(e_{(19,6)}\|T)=$ $r(e_{(19,7)}\|T)=r(e_{(19,8)}\|T)=r(e_{(19,9)}\|T)$ $r(e_{(20,1)}\|T)=r(e_{(20,2)}\|T)=r(e_{(20,3)}\|T)=r(e_{(20,4)}\|T)=$ $r(e_{(20,5)}\|T)$ $r(e_{(21,1)}\|T)=r(e_{(21,2)}\|T)=r(e_{(21,3)}\|T)=r(e_{(21,4)}\|T)=$ $r(e_{(21,5)}\|T)$

Table 2: Comparison of vertices for different cases

After generalizing
we have
$r(e_{(2n+4,3)}|T)=r(e_{(2n+4,2)}|T)$,

$r(e_{(2n+6,4)}|T)=r(e_{(2n+6,6)}|T)$,

$r(e_{(2n+1,3)}|T)=r(e_{(2n+1,2)}|T)=r(e_{(2n+1,1)}|T)$,
$r(e_{(2n+1,3)}|T)=r(e_{(2n+1,4)}|T)$,

These are contradictions. Hence, the edge EMD of the carbon nanotube is 3.

The investigation into the MD and EMD of h-BN and CNTs yields crucial insights into the structural and functional properties of these nanomaterials. The consistent MD

of 2 for h-BN implies that only two distinct points are required to uniquely identify any other point in the structure, elucidating its inherent simplicity in terms of navigation and localization. This characteristic is invaluable in various applications, including nanoelectronics and photonics, where precise positioning and routing of signals are paramount. Furthermore, the EMD of 2 underscores the efficiency of pathways along the edges of the h-BN lattice, accentuating its potential to facilitate fast and reliable information transfer within nanodevices. Similarly, the metric and EMDs of 3 for CNTs shed light on their more intricate spatial organization compared to h-BN. With three points necessary for pinpointing any location within the CNT structure, this indicates a higher degree of complexity, which can be advantageous in applications demanding greater degrees of freedom in manipulation and assembly, such as in nanorobotics and drug delivery systems.

Understanding the metric and EMDs of h-BN and CNTs not only provides fundamental insights into their geometric properties but also paves the way for optimizing their performance in diverse technological realms. By harnessing the minimalistic yet effective navigation offered by h-BN, engineers, and researchers can devise innovative strategies for designing next-generation nanoelectronic circuits and optoelectronic devices with enhanced functionality and reliability. Meanwhile, the slightly higher dimensions observed in CNTs offer a versatile platform for exploring novel applications requiring more intricate spatial arrangements, ranging from advanced sensing technologies to targeted drug delivery systems. Ultimately, this investigation underscores the importance of geometric characterization in unlocking the full potential of nanomaterials, guiding the development of tailored solutions for a myriad of scientific and technological challenges.

3. Conclusion

This study reveals that hexagonal boron nitride (h-BN) has an MD and EMD of 2, while carbon nanotubes (CNTs) have an MD and EMD of 3. These findings highlight the unique structural properties of these nanomaterials, with implications for various technological applications. Understanding their EMD offers valuable insights into their geometry and potential for tailored functionalization, driving advancements in nanoscience and engineering.

Acknowledgements

The authors thank the readers of the European Journal of Pure and Applied Mathematics, for making our journal successful.

References

[1] Ali Ahmad, Martin Bača, and Saba Sultan. Computing the metric dimension of kayak paddles graph and cycles with chord. *Proyecciones (Antofagasta)*, 39(2):287–300, 2020.

[2] Muhammad Ahsan, Zohaib Zahid, Sohail Zafar, Arif Rafiq, M Sarwar Sindhu, and Muhammad Umar. Computing the edge metric dimension of convex polytopes related graphs. *J. Math. Comput. Sci*, 22:174–188, 2021.

[3] Imtiaz Ali, Muhammad Javaid, and Yilun Shang. Computing dominant metric dimensions of certain connected networks. *Heliyon*, 10:e25654, 2024.

[4] Murtaza Ali, Gohar Ali, Muhammad Imran, Abdul Qudair Baig, and Muhammad Kashif Shafiq. On the metric dimension of mobius ladders. *Ars Comb.*, 105:403–410, 2012.

[5] Gary Chartrand, Linda Eroh, Mark A Johnson, and Ortrud R Oellermann. Resolvability in graphs and the metric dimension of a graph. *Discrete Applied Mathematics*, 105(1-3):99–113, 2000.

[6] Vasek Chvátal. Mastermind. *Combinatorica*, 3:325–329, 1983.

[7] Paul Erdos and Alfréd Rényi. On two problems of information theory. *Magyar Tud. Akad. Mat. Kutató Int. Közl*, 8(1-2):229–243, 1963.

[8] Frank Harary and Robert A Melter. On the metric dimension of a graph. *Ars combinotria*, 2(1):191–195, 1976.

[9] Aleksander Kelenc, Niko Tratnik, and Ismael G Yero. Uniquely identifying the edges of a graph: the edge metric dimension. *Discrete Applied Mathematics*, 251:204–220, 2018.

[10] Samir Khuller, Balaji Raghavachari, and Azriel Rosenfeld. Landmarks in graphs. *Discrete applied mathematics*, 70(3):217–229, 1996.

[11] Ali NA Koam and Ali Ahmad. Barycentric subdivision of cayley graphs with constant edge metric dimension. *IEEE Access*, 8:80624–80628, 2020.

[12] Dorota Kuziak. Strong resolvability in product graphs. In *1st URV Doctoral Workshop in Computer Science and Mathematics*, page 41. Publicacions URV, 2014.

[13] Bernt Lindström. On a combinatory detection problem i. *A Magyar Tudományos Akadémia Matematikai Kutató Intézetének Közleményei*, 9(1-2):195–207, 1964.

[14] Jia-Bao Liu, Muhammad Faisal Nadeem, Hafiz Muhammad Afzal Siddiqui, and Wajiha Nazir. Computing metric dimension of certain families of toeplitz graphs. *IEEE Access*, 7:126734–126741, 2019.

[15] Jia-Bao Liu, Ali Zafari, and Hassan Zarei. Metric dimension, minimal doubly resolving sets, and the strong metric dimension for jellyfish graph and cocktail party graph. *Complexity*, 2020:1–7, 2020.

[16] Ali Murtaza, Ali Gohar, Ali Usman, and Rahim MT. On cycle related graphs with constant metric dimension. *Open journal of discrete mathematics*, 2012, 2012.

[17] Futaba Okamoto, Bryan Phinezy, and Ping Zhang. The local metric dimension of a graph. *Mathematica Bohemica*, 135(3):239–255, 2010.

[18] Hassan Raza and Ying Ji. Computing the mixed metric dimension of a generalized petersen graph p (n, 2). *Frontiers in Physics*, 8:211, 2020.

[19] Hassan Raza, Ying Ji, and Shaojian Qu. On mixed metric dimension of some path related graphs. *IEEE Access*, 8:188146–188153, 2020.

[20] Hassan Raza, Jia-Bao Liu, and Shaojian Qu. On mixed metric dimension of rotationally symmetric graphs. *IEEE Access*, 8:11560–11569, 2019.

[21] Zahid Raza and MS Bataineh. The comparative analysis of metric and edge metric dimension of some subdivisions of the wheel graph. *Asian-European Journal of Mathematics*, 14(04):2150062, 2021.

[22] Laxman Saha, Bapan Das, Kalishankar Tiwary, Kinkar Chandra Das, and Yilun Shang. Optimal multi-level fault-tolerant resolving sets of circulant graph $c(n : 1, 2)$. *Mathematics*, 11(8):1896, 2023.

[23] Laxman Saha, Rupen Lama, Kalishankar Tiwary, Kinkar Chandra Das, and Yilun Shang. Fault-tolerant metric dimension of circulant graphs. *Mathematics*, 10(1):124, 2022.

[24] Peter J Slater. Leaves of trees. *Congr. Numer*, 14(37):549–559, 1975.

[25] Bin Yang, Muhammad Rafiullah, Hafiz Muhammad Afzal Siddiqui, and Sarfraz Ahmad. On resolvability parameters of some wheel-related graphs. *Journal of Chemistry*, 2019:1–9, 2019.

[26] Ismael González Yero. Vertices, edges, distances and metric dimension in graphs. *Electronic Notes in Discrete Mathematics*, 55:191–194, 2016.

[27] Awais Yousaf, Hanan Alolaiyan, Muhammad Nadeem, and Abdul Razaq. Retracted article: Topological analysis of carbon and boron nitride nanotubes. *Scientific reports*, 10(1):1–9, 2020.

[28] Yuezhong Zhang and Suogang Gao. On the edge metric dimension of convex polytopes and its related graphs. *Journal of Combinatorial Optimization*, 39(2):334–350, 2020.